

Characterization of the scatter component in large axial field-of-view PET scanners: a Monte Carlo simulation study

Amir Ghabrial, Daniel Franklin and Habib Zaidi[†], *IEEE Fellow*

Abstract— A simulation study was conducted to estimate the scatter fraction (SF) and to determine the most suitable line source radial offset displacement required to measure the SF for the total body long axial field-of-view (LAFOV) PET scanner by simulating different cylindrical and anthropomorphic digital phantoms. Simulations are conducted using a scanner model together with scatter phantoms adapted from the NEMA NU-2 2007 scatter phantom design, modified to suit the dimensions of the respective scanners, with line sources of various activities placed at a 45 mm radial offset. SF estimates obtained using the NEMA protocol are compared to values obtained with uniformly filled water phantom of the same length. A whole-body study is conducted using a set of 12 anthropomorphic phantoms with different BMIs, with different organs and anatomical structures filled with realistic concentrations of ¹⁸F-FDG. The SF obtained at 45 mm radial offset using 1 kBq/ml with the 200 cm (LAFOV scanner) and 70 cm (mCT) cylindrical phantoms are 40.07% and 34.35%, respectively. In both cases, a comparison with the SF estimate obtained with a uniformly filled cylindrical phantom shows that the NEMA NU2-2007 phantom with the line source positioned at the recommended radial offset of 45 mm significantly overestimates the SF. Instead, it was found that for both scanners, the optimal radial offset for accurate estimation of the SF was approximately 60 mm. High SF correlation coefficients were obtained between the SFs estimated with anthropomorphic phantoms with realistic biodistribution of ¹⁸F-FDG and an equivalent volume cylindrical phantom for the LAFOV PET scanner; in addition, BMI was strongly positively correlated with SF. The SF is found to be higher for the LAFOV compared with the mCT PET scanner. The optimal radial displacement for a LAFOV PET scanner using a NEMA-like phantom was found to be 60 mm, compared to the value of 45 mm suggested by the NEMA protocol.

Index Terms—PET, scatter fraction, total-body scanner

I. INTRODUCTION

The scatter fraction (SF) of a PET scanner is an important performance characteristic, which quantifies the sensitivity of the PET scanner relative to the scattered radiation. It is a function of several physical and geometric parameters, such as the scintillation detector energy resolution and window, detector geometry and solid angle coverage; it also depends on the size and density of the imaging subject. One significant recent trend in PET system development has been the growing interest in whole-body PET, in which the axial field-of-view

(FOV) is extended to cover the full length of an adult human (typically around two meters). Such long axial field-of-view scanners offer numerous benefits compared to classical short axial field-of-view scanners.

In this work, the scatter fraction for a long axial FOV (LAFOV) PET scanner based on EXPLORER [1] is evaluated using Monte Carlo simulations in the Geant4 Application for Tomographic Emission (GATE), and compared to that of a conventional mCT PET system using a variety of scattering phantoms based on variants of those used in the NEMA NU-2 2007 protocol. Several modifications to the existent NEMA NU2-2007 standard which aim to improve the accuracy of the estimated scatter fraction are proposed based on previous work [2] and evaluated for both the mCT and LAFOV scanner designs.

II. METHODS

The simulated LAFOV PET scanner geometry replicates the design of the EXtreme Performance Long REsearch scanner (EXPLORER) [3]. Its ring diameter is 80~cm, transaxial FOV 70~cm and it has 36 axial block rings which give an AFOV of 197~cm. Each ring consists of has 48 detector blocks. Each detector block contains an array of 15×15 LSO scintillation crystals, each 3.34mm×3.34mm×20mm. The crystal pitch is 3.42 mm, with the 0.08 mm gap between adjacent crystals representing the powder based reflector. The simulated LAFOV PET scanner has an energy resolution of 13%, and uses the same energy window as the mCT scanner (435~keV LLD, 650 keV ULD). The coincidence timing window is set to 5.5ns, and time-of-flight (TOF) resolution is 530 ps.

An anthropomorphic phantom model based on the standard ICRP human phantom was used to produce a set of realistic voxelised human 4D phantoms with a range of body mass index (BMI) values [4]. These models were then used with GATE for scatter fraction studies on the LAFOV PET scanner. Unlike the cylindrical NEMA phantoms, the anthropomorphic digital phantoms comprise organs and anatomical structures and have complex activity distributions based on realistic whole-body uptake of ¹⁸F-FDG. The phantom includes fourteen different organs and anatomical structures.

III. RESULTS AND DISCUSSION

The scatter fraction for the mCT PET scanner calculated using simulations performed with the standard NEMA phantom and an energy window of 435-650~keV was 34.35%. This result is consistent with NEMA results obtained in a previously-published experimental study using a source activity of 1~kBq/ml. The modified NEMA simulations (with a 200~cm phantom and a source activity of 1~kBq/ml) with a radial offset of 45~mm for the LAFOV PET scanner indicated

A. Ghabrial is with the Division of Nuclear Medicine and Molecular Imaging, Geneva University Hospital, Switzerland. D. Franklin is with the University of Technology Sydney, Australia.

[†]H. Zaidi is with the Division of Nuclear Medicine and Molecular Imaging, Geneva University Hospital, CH-1211 Geneva, Switzerland, Geneva University Neurocenter, CH-1205 Geneva, Switzerland. He is also with the Department of Nuclear Medicine and Molecular Imaging, University of Groningen, University Medical Center Groningen, Groningen, Netherlands, and the Department of Nuclear Medicine, University of Southern Denmark, DK-500, Odense, Denmark (e-mail: habib.zaidi@hcu.ch).

that the SF was approximately 40.0%. Comparing these results to the ground truth values obtained using the uniformly-filled cylindrical phantom indicates that the results obtained with the NEMA/NEMA-like phantom with a 45~mm offset significantly overestimate the SF value. The SF curve intersects the uniform phantom value at a radial displacement of approximately 80~mm, which is the same displacement as that previously reported as being optimal for the GE Discovery STE scanner [2]. On the other hand, following a similar method to [2], the SF curve intersects with the mean SF value obtained from all of the simulations of different radial displacements at about 60~mm radial displacement from the phantom center, for both the mCT and the LAFOV PET scanners, as illustrated in Fig. 1 (a) et (b), respectively. The scatter fractions obtained for uniformly-filled NEMA-like phantoms with diameters of between 100 and 600 mm and lengths of 70 and 200 cm for the simulated mCT and LAFOV PET scanners, respectively, are shown in Fig. 2 together with a fitted second-order polynomial.

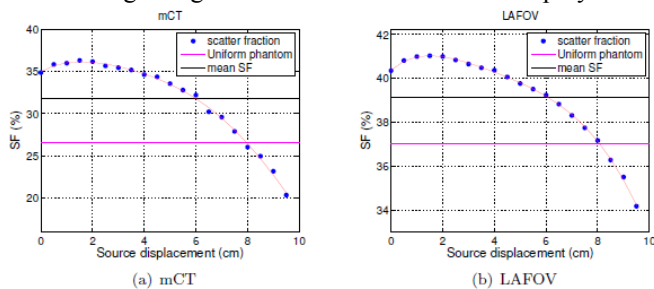


Fig. 1. Plots of scatter fraction as a function of the source displacement, obtained using NEMA/NEMA-like polyethylene phantoms with diameters of 200 mm and lengths of 70 cm and 200 cm for the mCT and LAFOV PET scanners, respectively.

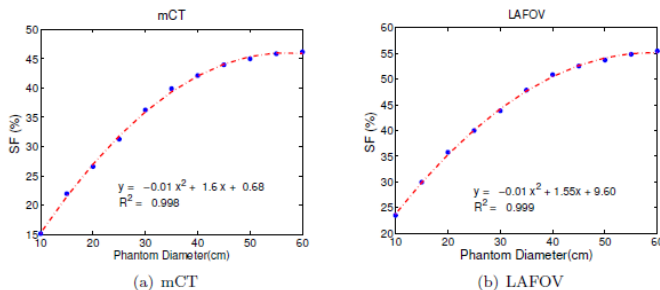


Fig. 2. Scatter fraction vs. diameter of uniformly filled NEMA/NEMA-like phantoms (70 cm and 200 cm for the mCT and LAFOV scanners, respectively). The results are fitted using a second polynomial.

The investigation demonstrated that estimation of the scatter fraction using the phantoms recommended in the NEMA NU-2-2007 overestimates the true value when the line source is located at a radial offset of 45~mm. The design of the NEMA phantom assumes a relatively short axial FoV compared to the length of the phantom. The simulation-based evaluation of optimal radial line-source displacement of the line source inserted in a solid polyethylene phantom in order to calculate the SF precisely corresponding to a uniform phantom of the same size resulted at approximately 80% of the phantom radius (80~mm) for both the mCT and LAFOV PET scanners. A strong positive correlation was found between the scatter fractions obtained with the anthropomorphic phantoms and equivalent-volume cylindrical phantoms for both the mCT and LAFOV PET scanners; slightly weaker correlation between the

BMIs of the anthropomorphic phantoms and the scatter fraction was also observed (Fig. 3). This is essentially the same result the same as reported for the GE Discovery STE scanner [2].

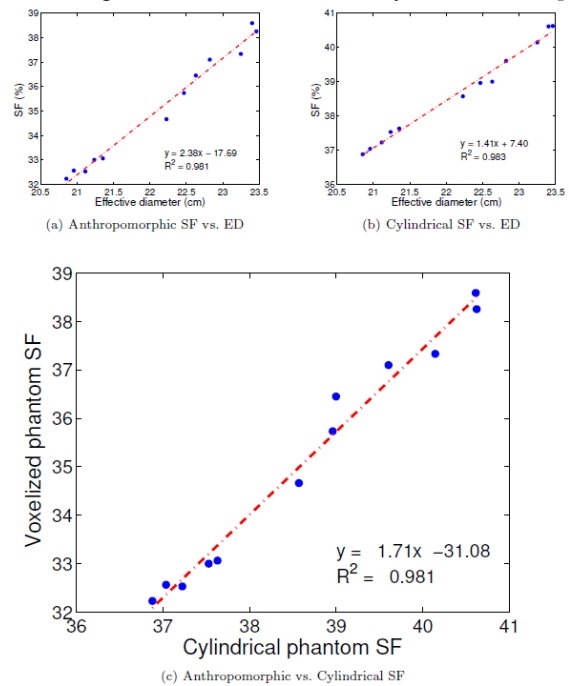


Fig. 3. Plots of scatter fractions obtained with voxelised anthropomorphic scatter phantoms and corresponding cylindrical phantoms, expressed as a function of effective diameter. The correlation between the scatter fractions obtained for both phantom types is also shown.

IV. CONCLUSION

A simulation study was performed to estimate the scatter fraction for the LAFOV PET scanner by simulating different cylindrical and anthropomorphic digital phantoms to characterize the scatter fraction within the total body imaging scanner. Twelve cylindrical phantoms was simulated, each with length of 200~cm, and diameters equal to the effective diameter for each of the twelve anthropomorphic phantoms containing organs filled with realistic ^{18}F -FDG activity concentrations. The SF increases as the object size increase; high correlation is observed between the scatter fraction obtained with anthropomorphic phantoms and an equivalent-volume cylindrical phantom for the LAFOV PET scanner.

ACKNOWLEDGMENT

This work was supported by the Swiss National Science Foundation under Grant No. SNSF 320030_176052.

REFERENCES

- [1] S. R. Cherry, T. Jones, J. S. Karp, J. Qi, W. W. Moses, and R. D. Badawi, "Total-body PET: Maximizing sensitivity to create new opportunities for clinical research and patient care.," *J Nucl Med*, vol. 59, no. 1, pp. 3-12, 2018.
- [2] A. Ferrero, J. K. Poon, A. J. Chaudhari, L. R. MacDonald, and R. D. Badawi, "Effect of object size on scatter fraction estimation methods for PET- A computer simulation study.," *IEEE Trans Nucl Sci*, vol. 58, no. 1, pp. 82-86, 2011.
- [3] J. K. Poon *et al.*, "Optimal whole-body PET scanner configurations for different volumes of LSO scintillator: a simulation study.," *Phys Med Biol*, vol. 57, no. 13, pp. 4077-4094, 2012.

- [4] A. Akhavanallaf, T. Xie, and H. Zaidi, "Development of a library of adult computational phantoms based on anthropometric indexes," *IEEE Trans Rad Plasma Med Sci* vol. 3, pp. 65-75, 2019.